Molecular Evolution of the Meiotic Recombination Pathway in Mammals

Investigations

Amy L. Dapper[1,2*] and Bret A. Payseur[1]

[1] Laboratory of Genetics, University of Wisconsin, Madison, WI 53706, USA

[2] Department of Biological Sciences, Mississippi State University, Mississippi State, MS 39762, USA

Running Title: Evolution of the Recombination Pathway

Keywords: (up to 5)

* Corresponding Author : Amy L. Dapper

Address: 295 E. Lee Blvd., P.O. Box GY, Mississippi State, MS 39762

Phone: (662) 325-7575

Email: dapper@biology.msstate.edu

Abstract

Meiotic recombination, the exchange of genetic material between homologous chromosomes during meiosis, is required for successful gametogenesis in most sexually reproducing species. Recombination is also a fundamental evolutionary force, influencing the fate of new mutations and determining the genomic scale over which selection shapes genetic variation. Despite the central importance of recombination, basic questions about its evolution have yet to be addressed. Although many genes that play roles in recombination have been identified, the molecular evolution of most of these genes remains uncharacterized. Using a phylogenetic comparative approach, we measure rates of evolution in 32 recombination pathway genes across 16 mammalian species, spanning primates, murids, and laurasithians. By analyzing a carefully-selected panel of genes involved in key components of recombination – spanning double strand break formation, strand invasion, the crossover/non-crossover decision, and resolution – we generate a comprehensive picture of the evolution of the recombination pathway in mammals. Recombination genes exhibit marked heterogeneity in the rate of protein evolution, both across and within genes. We report signatures of rapid evolution and positive selection that could underlie species differences in recombination rate. [**NEEDS WORK HERE**]

Abstract Word Count : (< 250)

Introduction

The reciprocal exchange of DNA between homologous chromosomes during meiosis – recombination – is required for successful gametogenesis in most species that reproduce sexually (Hassold and Hunt 2001). The rate of recombination is a major determinant of patterns of genetic diversity in populations, influencing the fate of new mutations (Hill and Robertson 1966), the efficacy of selection (Felsenstein 1974; Charlesworth *et al.* 1993; Comeron *et al.* 1999; Gonen *et al.* 2017), and important features of the genomic landscape (Begun and Aquadro 1992; Charlesworth *et al.* 1994; Duret and Arndt 2008).

Although recombination rate is often treated as a constant, this fundamental parameter evolves over time. Genomic regions ranging in size from short sequences to entire chromosomes vary in recombination rate – both within and between species (Burt and Bell 1987; Broman *et al.* 1998; Jeffreys *et al.* 2005; Coop and Przeworski 2007; Kong *et al.* 2010; Dumont *et al.* 2011; Smukowski and Noor 2011; Comeron *et al.* 2012; Segura *et al.* 2013; Dapper and Payseur 2017; Stapley *et al.* 2017).

Genome-wide association studies are beginning to reveal the genetic basis of differences in recombination rate within species. Individual recombination rates have been associated with variation in specific genes in populations of *Drosophila melanogaster* (Hunter *et al.* 2016), humans (Kong *et al.* 2008, 2014; Chowdhury *et al.* 2009; Fledel-Alon *et al.* 2011), domesticated cattle (Sandor *et al.* 2012; Ma *et al.* 2015; Kadri *et al.* 2016; Shen *et al.* 2018), domesticated sheep (Petit *et al.* 2017), Soay sheep (Johnston *et al.* 2016), and red deer (Johnston *et al.* 2018). Variants in several of these genes correlate with recombination rate in multiple species, including: *Rnf212* (Kong *et al.* 2008; Chowdhury *et al.* 2009; Fledel-Alon *et al.* 2011; Sandor *et al.* 2012; Johnston *et al.* 2016; Kadri *et al.* 2016; Petit *et al.* 2017), *Rnf212B* (Johnston *et al.* 2016, 2018; Kadri *et al.* 2016), *Rec8* (Sandor *et al.* 2012; Johnston *et al.* 2016, 2018), *Hei10/Ccnb1ip1* (Kong *et al.* 2014; Petit *et al.* 2017), *Msh4* (Kong *et al.* 2014; Ma *et al.* 2015; Kadri *et al.* 2016; Shen *et al.* 2018), *Cplx1* (Kong *et al.* 2014; Ma *et al.* 2015; Johnston *et al.* 2016; Shen *et al.* 2018) and *Prdm9* (Fledel-Alon *et al.* 2011; Sandor *et al.* 2012; Kong *et al.* 2014; Ma *et al.* 2015; Shen *et al.* 2018).

In contrast, the genetics of recombination rate variation among species remains poorly understood. Divergence at the di-cistronic gene *mei-217/mei-218* explains much of the disparity in genetic map length between *D. melanogaster* and *D. mauritiana* (Brand *et al.* 2018). *mei-217/mei-218* is the only gene known to confer a recombination rate difference between species, though quantitative trait loci that contribute to shifts in rate among subspecies of house mice have been identified (Dumont and Payseur 2010; Murdoch *et al.* 2010; Balcova *et al.* 2016).

One strategy for understanding how species diverge in recombination rate is to inspect patterns of molecular

evolution at genes involved in the recombination pathway. This approach incorporates knowledge of the molecular and cellular determinants of recombination and is motivated by successful examples. *mei-217/mei-218* was targeted for functional analysis based on its profile of rapid evolution between *D. melanogaster* and *D. mauritiana* (Brand *et al.* 2018). *Prdm9*, a protein that positions recombination hotspots in house mice and humans through histone methylation (Myers *et al.* 2010; Parvanov *et al.* 2010; Grey *et al.* 2011, Paigen2018; 2018), shows accelerated divergence across mammals (Oliver *et al.* 2009). The rapid evolution of *Prdm9* – which localizes to its zinc-finger DNA binding domain (Oliver *et al.* 2009) – appears to be driven by selective pressure to recognize new hotpot motifs as old ones are destroyed via biased gene conversion (Myers *et al.* 2010; Ubeda and Wilkins 2011; Lesecque *et al.* 2014; Latrille *et al.* 2017). Although these examples demonstrate the promise of signatures of molecular evolution for illuminating recombination rate differences between species, patterns of divergence have yet to be reported for most genes involved in meiotic recombination.

Mammals provide a useful system for dissecting the molecular evolution of the recombination pathway for several reasons. First, the evolution of recombination rate has been measured along the mammalian phylogeny (Dumont and Payseur 2008; Segura *et al.* 2013). Second, recombination rate variation has been associated with specific genes in mammalian populations (Kong *et al.* 2008, 2014; Chowdhury *et al.* 2009; Sandor *et al.* 2012; Ma *et al.* 2015; Johnston *et al.* 2016, 2018; Kadri *et al.* 2016; Petit *et al.* 2017; Shen *et al.* 2018). Third, laboratory mice have proven to be instrumental in the identification and functional characterization of recombination genes (Vries *et al.* 1999; Baudat *et al.* 2000; Romanienko and Camerini-Otero 2000; Yang *et al.* 2006; Ward *et al.* 2007; Schramm *et al.* 2011; Bisig *et al.* 2012; Bolcun-Filas and Schimenti 2012; La Salle *et al.* 2012; Kumar *et al.* 2015; Finsterbusch *et al.* 2016; Stanzione *et al.* 2016) .

Work in mice indicates that the mammalian recombination pathway is roughly divided into five major steps, each of which is regulated by a handful of genes. The first step is the formation of hundreds of double strand breaks (DSBs) throughout the genome (Bergerat *et al.* 1997; Keeney *et al.* 1997; Baudat *et al.* 2000; Romanienko and Camerini-Otero 2000; Baudat and Massy 2007; Finsterbusch *et al.* 2016; Lange *et al.* 2016). After formation, DSBs are identified, processed, and paired with their corresponding location on the homologous chromosome through the processes of homology search and strand invasion (Keeney 2007; Cloud *et al.* 2012; Brown and Bishop 2014; Finsterbusch *et al.* 2016; Kobayashi *et al.* 2016; Oh *et al.* 2016; Xu *et al.* 2017). The pairing of homologous chromosomes is then stabilized by a proteinaceous structure referred to as the synaptonemal complex (SC) (Meuwissen *et al.* 1992; Schmekel and Daneholt 1995; Costa *et al.* 2005; Vries *et al.* 2005; Hamer *et al.* 2006; Yang *et al.* 2006; Schramm *et al.* 2011; Fraune *et al.* 2014; Hernández-Hernández *et al.* 2016). The SC also forms a substrate on which the eventual crossover

events will take place [**citations**]. It is at this point that a small subset of DSBs is designated to mature into crossovers, leaving the majority of DSBs to be resolved as non-crossovers (Snowden *et al.* 2004; Yang *et al.* 2008; Reynolds *et al.* 2013; Finsterbusch *et al.* 2016; Rao *et al.* 2017). Finally, this designation is followed, and each DSB is repaired as a crossover or a non-crossover (Baker *et al.* 1996; Edelmann *et al.* 1996; Lipkin *et al.* 2002; Rogacheva *et al.* 2014; Xu *et al.* 2017).

In this article, we examine the molecular evolution of 32 key recombination genes, evenly distributed across each major step in the recombination pathway, in 16 mammalian species spanning Primates, Rodents and Laurasiatherians. In addition to revealing patterns of divergence across diverse mammalian species, we leverage human polymorphism data to make robust evolutionary inferences. Our results provide a comprehensive picture of evolution in the recombination pathway in mammals and identify steps of the pathway most likely to contribute to differences in recombination rate between species.

Materials and Methods

Data Acquisition & Processing

We selected a focal panel of 32 recombination genes (See Table1). The panel was constructed to: (1) cover each major step in the recombination pathway as evenly as possible, (2) contain genes that have integral functions in each step, and (3) include genes that have been associated with inter-individual differences in recombination rate within mammalian populations. Reference sequences were downloaded for each gene in 16 110 mammalian species from both NCBI and Ensembl (Release-89)(Wheeler *et al.* 2006; Zerbino *et al.* 2017).

Alternative splicing is widespread and presents a challenge for molecular evolution studies (Pan *et al.* 2008; Barbosa-Morais *et al.* 2012). To focus our analyses on coding sequences that are transcribed during meiosis and to validate the computational annotations for each gene in each species, we used available testes expression datasets. We downloaded raw testes expression data for each mammalian species from NCBI Gene Expression Omnibus (GEO) (Table S1)(Barrett *et al.* 2012). We converted the SRA files into FASTQ files using SRAtoolkit (Leinonen *et al.* 2010). The reads were mapped to an indexed reference genome (Table S2,3) (Bowtie2, (Langmead and Salzberg 2012)) using TopHat (Trapnell *et al.* 2009). The resulting bam files were sorted using Samtools (Li *et al.* 2009) and visualized using IGV 2.4.10 (Thorvaldsdóttir *et al.* 2013). This allowed us to: (1) identify the transcript expressed in testes, (2) check the reference transcript for errors, and (3) revise the reference transcript based upon the transcript data.

We compared expression data to annotations from both Ensembl and NCBI (Wheeler *et al.* 2006; Zerbino *et*

al. 2017). When both transcripts were identical, we selected the NCBI transcript. The Ensembl transcript was used instead when: (1) the NCBI reference sequences was not available for a given gene in a given species, (2) when none of the NCBI transcripts matched the expression data, or (3) when there were sequence differences between the two transcripts and the Ensembl transcript was more parsimonious - i.e. had the fewest differences when compared to the rest of sequences in the alignment. The use of testes expression data was a key data processing step and the inclusion of species in this study was primarily determined by the availability of testes expression data.

Phylogenetic Comparative Approach in Mammals

For each gene, we used phylogenetic analysis by maximum likelihood (PAML 4.8) to measure the rate of evolution across the mammalian phylogeny and to search for molecular signatures indicative of positive selection (Table 2) (Yang 1997, 2007). This approach requires a sequence alignment and a phylogenetic tree. For each gene, sequences were aligned using Translator X, a codon-based alignment tool, powered by MUSCLE v3.8.31 (Edgar 2004; Abascal *et al.* 2010). Each alignment was examined by hand and edited as necessary. We used a species tree that reflects current understanding of the phylogenetic relationships of the species included in our study (Figure 1)(Prasad *et al.* 2008; Perelman *et al.* 2011; Fan *et al.* 2013; Chen *et al.* 2017).

Due to the ambiguity in the relationship between Laurasithians and the placement of tree shrews, we also inferred gene trees using MrBayes (Ronquist *et al.* 2012; Fan *et al.* 2013; Chen *et al.* 2017). This approach also allowed us to control for effects of incomplete lineage sorting (ILS) (Pamilo and Nei 1988; Rosenberg 2002; Scornavacca and Galtier 2017). Using gene trees and using the consensus species tree produced highly similar results (Table S4).

For the majority of genes, transcripts from all 16 species were used (19 genes). However, for a number of genes, the chimpanzee and bonobo sequences were identical, in which case only the chimpanzee sequence was included in the analyses (11 genes). In one case, the chimpanzee, bonobo and human sequences were all identical, in which case only the human sequence was included in the analyses. In only a small number of instances, a suitable reference sequence could not be identified for a given species.

We estimated rates of synonymous and non-synonymous substitutions per site using the CODEML program in PAML4.8 (Yang 2007). This program considers multiple substitutions per site, different rates of transitions and transversions, and effects of codon usage (Yang 2007). Rates of substitution were computed for 6 different models of molecular evolution (Table 2). The fit of each model was compared using a likelihood ratio test.

Reported substitution rates assume the best-fit model for each gene.

Identifying Signatures of Selection

To test for positive selection, we compared the fit of models including a class of sites with ω greater than 1 to the fit of models in which all classes of sites have ω values equal to, or less than, 1. Specifically, we report three comparisons: M1 vs. M2, M7 vs. M8, M8 vs. M8a (Table 2). The first comparison, M1 vs. M2, compares a model with two classes of sites ($\omega < 1$, $\omega = 1$) to a model with a third class of sites where ω is greater than 1, indicative of positive selection (Yang 2007). More complex models (M7 & M8) were developed to take into account variation in ω less than one among sites within genes and thus, include 10 site classes drawn from a beta distribution between 0 and 1 (Yang 2007). In this case, Model 8 includes an additional 11 class of sites in which ω is greater than 1, allowing for the identification of signatures of positive selection (Yang 2007). In cases in which a large fraction of sites within a gene are evolving neutrally ($\omega = 1$), Model 8 will fit significantly better due to a very poor fit of Model 7 rather than a signature of positive selection. To avoid incorrectly identifying signature of positive selection, Model 8 is also compared to Model 8a which contains a larger fraction of neutrally evolving sites than Model 7 [**citations**]. We also report the number of significant Bayes-Empirical-Bayes (BEB) ω estimates for individual codons in each gene.

Multinucleotide Mutations

Multi-nucleotide mutations (MNMs) occur when two mutations happen simultaneously in close proximity (Schrider *et al.* 2011; Besenbacher *et al.* 2016). MNMs violate the PAML assumption that the probability of two simultaneous mutations in the same codon is 0 (Yang 2007; Venkat *et al.* 2018). Recent work has shown that MNMs can falsely detect positive selection when using branch-site tests in PAML (Venkat *et al.* 2018). Although we did not use branch-site tests, it is possible that MNMs contributed to some of the signatures of positive selection we observed. We could not directly identify MNMs in our dataset. Instead, we identified codons with multiple differences (CMDs) that likely arose on a single branch of the phylogeny. We used PAML to reconstruct the ancestral sequence at each node in the phylogeny (Yang 2007). For the reconstruction, Model 8 was chosen because we specifically re-analyzed genes that showed evidence for positive selection when comparing Model 7 with Model 8. From the ancestrally reconstructed sequences, we identified any codons in which PAML inferred more than 1 substitution on a single branch. All identified CMDs were removed from the sequences in which they occurred. For example, if a CMD was identified in an external branch, that codon was replaced with '—' only in the sequence of that species. If a CMD was inferred on an

internal branch, the codon was replaced with '—' in all species descended from that internal branch. For each gene that showed evidence of positive selection using the unedited sequences, we also conducted PAML analyses using sequences from which all CMDs were removed.

Polymorphism & Divergence in the Primate Lineage

To further examine evidence for selection on recombination genes, we compared divergence between humans and macaque to polymorphism within humans in the recombination genes. Human polymorphism data was downloaded from ExAC database (Lek *et al.* 2016). The ExAC database spans 60,706 unrelated individuals sequenced as part of both disease-specific and population genetic studies (Lek *et al.* 2016). To avoid biases introduced by population structure, we restricted our analyses to the population with the largest representation in the database: European, non-Finnish, individuals (N = 33,370)(Lek *et al.* 2016). Polymorphism data for the correct transcript of RNF212 (based upon expression data) was not available in the ExAC database, and thus this gene was not included in this analysis.

We compared counts of non-synonymous and synonymous polymorphisms to counts of non-synonymous and synonymous substitutions using the McDonald-Kreitman test (McDonald and Kreitman 1991). The neutral expectation is that the ratio of non-synonymous to synonymous substitutions is equal to the ratio of non-synonymous to synonymous polymorphisms (McDonald and Kreitman 1991). Significant deviations can provide evidence of positive or negative selection. The neutrality index (NI) measures the direction and degree of departures from the neutral expectation (Charlesworth 1994). A NI of less than one is indicative of positive selection and the fraction of adaptive amino acid substitutions can be estimated as 1 - NI (Charlesworth 1994; Fay *et al.* 2001; Smith and Eyre-Walker 2002). We also measure the direction of selection (DoS) for each gene, an additional statistic that measures the direction and degree of neutral expectations and has been shown to be less sensitive to bias than NI under certain conditions (Stoletzki and Eyre-Walker 2010). A positive DoS is consistent with positive selection, and vice versa (Stoletzki and Eyre-Walker 2010). Additionally, we estimated pairwise divergence (ω) between humans and macaques using the *yn00* package in PAML (Yang 2007).

Identifying Evolutionary Patterns

To identify evolutionary patterns among our recombination genes, we compared the rate of evolution and the proportion of genes experiencing positive selection among groups of interest. We asked: (1) Do genes that function in different steps of the pathway exhibit different rates of evolution? (2) Do genes that function

post-synapsis evolve more rapidly than genes that function pre-synapsis? and (3) Do genes associated with between-individual variation in recombination rate diverge more rapidly between species? All statistical analyses were performed in R [**citation**].

The evolutionary rate covariation (ERC) metric is the correlation coefficient between branch-specific rates between two proteins (Clark *et al.* 2012). ERC is frequently elevated among interacting proteins (Pazos and Valencia 2001; Hakes *et al.* 2007; Clark *et al.* 2009) and is assumed to result from: (1) concordance in fluctuating evolutionary pressures, (2) parallel evolution of expression level, or (3) compensatory changes between co-evolving genes (Clark *et al.* 2012, 2013). We used a publicly available ERC dataset (https://csb.pitt.edu/erc_analysis/index.php) to compare the median ERC-value among a subset of the focal recombination genes ($N = 25$) to other genes in the genome, as described in (Priedigkeit *et al.* 2015).

To control for an observed elevation in ERC among recombination genes and test for relationships between specific groups, we also conducted an ERC analysis that was restricted to the focal set of 32 recombination genes. Branch lengths were calculated using the *aaML* package in PAML (Yang 2007) and pairwise ERC values were calculated following the methods of (Clark *et al.* 2012). Using this approach, we specifically compared the ERC values among three of the most rapidly evolving recombination genes (*TEX11*, *SHOC1*, and *SYCP2*) to the rest of the recombination genes.

Results

Recombination genes evolve at different rates in mammals

We observed substantial heterogeneity in the rate of evolution of recombination genes, spanning a range of 0.0268 – 0.8483 (mean $\omega = 0.3275$, SD = 0.1971, median = 0.30945) (Figure 2A, Figure 3, Table 3). Four genes exhibit particularly rapid evolution compared to other recombination genes, with evolutionary rates greater than 1 SD above the mean (*IHO1*, *SHOC1*, *SYCP2*, *TEX11*). At the other end of the spectrum, five genes have evolutionary rates more than 1 SD below the mean and are highly conserved across the mammalian phylogeny (*BRCC3*, *DMC1*, *HEI10*, *RAD50*, *RAD51*). In general, there is very high concordance between evolutionary rate across mammals and pairwise divergence between humans and macaques (mean ω = 0.3301, SD = 0.2370, median = 0.30925)($\rho = 0.833774$, p = 3.11e-9, Spearman's correlation)(Figure 2B, Table 4). It should be noted, however, that these two measures are not independent - divergence between human and macaque sequences was incorporated in the phylogenetic analysis. In comparisons between human and macaque sequences, six genes have evolutionary rates more than 1 SD above the mean (*CNTD1*, *IHO1*, *MEI4*, *RAD21L*, *SHOC1*, *TEX11*) and six genes have evolutionary rates more than 1 SD below the mean (*DMC1*, *HORMAD1*, *MLH1*, *MRE11*, *RAD50*, *RAD51*).

The genes that show the most rapid and most conserved rates of divergence between humans and macaques are mostly the same genes that show extreme evolutionary rates across the mammalian phylogeny. Notable exceptions include *MEI4* ($\omega_{\text{mammals}} = 0.4332$, $\omega_{\text{human-macaque}} = 0.7252$), *CNTD1* ($\omega_{\text{mammals}} = 0.2496$, $\omega_{\text{human-macaque}} = 0.6803$), *HEI10* ($\omega_{\text{mammals}} = 0.1226$, $\omega_{\text{human-macaque}} = 0.3235$), and *HORMAD1* ($\omega_{\text{mammals}}$ = 0.3036, $\omega_{\text{human-macaque}} = 0.0901$.

Recombination genes evolve faster than other genes in primates

Gradnigo et al. (2016) measured the rate of divergence between human and macaque for 3,606 genes throughout the genome. We used this dataset to ask whether the rate of evolution of recombination genes as a group is different than expected from the genome-wide distribution. Mean rates for sets of 32 ω values randomly sampled from the 3,606-gene list rarely exceeded the mean rate for recombination genes (p = 0.0075, 10,000 random draws) (Figure 4), suggesting that recombination genes evolve faster on average.

Recombination genes display signatures of positive selection across mammals

Comparing polymorphism within humans to divergence between humans and macaques revealed an excess of non-synonymous polymorphisms at 16 genes (Fisher's Exact Test, Table 4). This pattern suggests the presence of weakly deleterious mutations at recombination genes in human populations. None of the recombination genes we surveyed had displayed a significant excess of non-synonymous substitutions, the expected signature of positive selection. Only one gene (*TEX11*) had a higher fraction ratio of non-synonymous to synonymous substitutions than non-synonymous to synonymous polymorphisms ($NI = 0.7879$; $DoS = 0.0534$)(Table 4). However, we did not observe higher allele frequencies among non-synonymous polymorphism than synonymous polymorphism, which is expected if most non-synonymous polymorphisms were weakly deleterious.

Comparative phylogenetic methods allow for the identification of signatures of selection acting on a subset of sites within a gene. We identified signatures of positive selection in 11 recombination genes (34.3%) using site models in *CODEML*. These genes include: *IHO1*, *MSH4*, *MRE11*, *NBS1*, *RAD21L*, *REC8*, *RNF212*, *SHOC1*, *SYCP1*, *SYCP2*, and *TEX11* (Table 2). For each of these genes, models that include a fraction of sites where the rate of non-synonymous substitutions is estimated to be greater than the rate of synonymous substitutions ($\omega > 1$, Model 8) fit better than models that did not include such a class of sites (Model 7, 8a). Due to the potential for multi-nucleotide mutations to produce false signatures of positive selection, we re-analyzed this subset of genes after removing any codons inferred to have accumulated multiple changes on a single branch (CMDs). After removing all CMDs, 1 gene (*TEX11*) retained a significant signature of positive selection (Table 5).

Recombination genes associated with inter-individual differences do not diverge more rapidly between species

Recombination genes previously associated with inter-individual differences in recombination rate do not evolve faster in mammals (average $\omega = 0.3943$ vs. average $\omega = 0.2925$, respectively; $p = 0.2381$, Mann-Whitney U Test), though the difference in evolutionary rates between these two classes of genes is greater when considering only divergence between humans and macaques (average $\omega = 0.4181$ vs. average $\omega = 0.2839$, respectively; $p = 0.08816$, Mann-Whitney U Test). Likewise, the proportion of recombination genes that exhibit signatures of positive selection is not higher among genes that have been associated with inter-individual differences (5/11 vs. 6/21; $p = 0.719$, **Fisher's Exact Test**).

A comparison among groups of genes assigned to six major steps in the recombination pathway yielded no significant differences (mammals: $p = 0.1422$, Kruskal-Wallis Test; human vs. macaque: $p = 0.2682$,

Kruskal-Wallis Test)(Figure 6). Similarly, genes acting before and after synapsis show similar evolutionary rates across mammals (average ω_before = 0.2723 vs. ω_after = 0.3762, $p = 0.1425$, Mann-Whitney U Test), though - again - the difference in evolutionary rates is greater when considering only divergence between humans and macaques (average ω_before = 0.2514 vs. ω_after = 0.3994, $p = 0.05827$, Mann-Whitney U Test).

Evolutionary rates among recombination genes are correlated

To determine the degree to which recombination genes exhibit correlated evolutionary rates across the mammalian phylogeny, we used a publicly available ERC database (https://csb.pitt.edu/erc_analysis/index.php) to measure pairwise ERC among recombination genes. Recombination genes show correlated evolutionary rates (mean ERC = 0.134) that are significantly higher than expected by randomly sampling the genome-wide distribution (permutation $p = 0.000358$).

TEX11, *SYCP2*, and *SHOC1* are three of the most rapidly evolving recombination genes among mammals (Table 3). Additionally, molecular genetics studies indicate that *TEX11* has direct protein-to-protein interactions with both *SHOC1* and *SYCP2* (Yang *et al.* 2008; Guiraldelli *et al.* 2018). *TEX11*, *SYCP2*, and *SHOC1* show correlated evolutionary rates (mean ERC = 0.42369) that are significantly higher than expected by randomly sampling among recombination genes (permutation $p = 0.025$).

Discussion

Observations about recombination genes as group:

We observed substantial variation in the rate of evolution of genes in the recombination pathway. However, there are a number of observations we can make about how recombination genes evolve as a group:

1) Rate correlations among recombination genes are higher than expected from rate correlations among other genes - evidence that the recombination pathway shapes the evolution of recombination genes.

2) In general, there is very high concordance between the rate of evolution of recombination genes in primates (human vs. macaque) and across the mammalian phylogeny, suggesting that the strength and direction of selection on recombination genes may be quite similar across mammals.

- Caveat: These two measures are not independent, divergence between humans and macaques is part of the measurement of divergence across mammals.

Note, there are some notable exceptions to the general concordance between the rate of evolution in primates and mammals – which may highlight genes that have experienced differences in the strength and direction of selection along the primate lineage.

- CNTD1, HORMAD1, and MEI4 have relatively average rates of evolution across the mammalian phylogeny. However, MEI4 and CNTD1 are among the most rapidly evolving recombination genes along the primate lineage, while HORMAD1 is one of the most conserved.

3) As a group, recombination genes tend to evolve more rapidly than other genes in primates. There are a couple of explanations as to why a group of genes may exhibited elevated rates of evolution:

- (1) Expression Level – genes with lower breadth of expression tend to evolve more rapidly. Recombination genes tend to be tissue-specific with low overall levels of expression. Sex-specific expression can also relax selection and elevate divergence. However, these genes are unlikely to be sex-specific as they affect recombination phenotypes in both sexes.
- (2) Positive Selection – it is possible that on average, recombination genes are more frequently subject to positive selection, elevating divergence between species.

Observations about groups of recombination genes:

1) We did not find evidence that genes previously associated with inter-individual variation in recombination rate show more rapid or adaptive evolution than other genes in the genome. There are two interpretations of this observation:

- (1) genes that produce inter-individual variation in recombination rate are unlikely to contribute to between species differences.
- (2) we did not detect an association because we have imperfect knowledge of the genes responsible for inter-individual variation.

2) We did not see a strong pattern that the rate of evolution of a gene could be predicted by the step in the pathway in which it functions. There are two interpretations of this observation:

- (1) The step of the recombination pathway a recombination functions in is not a good proxy for the selection pressures acting on a gene.
- (2) Due to the significant variation in evolutionary rates between genes, we do not have enough power to detect similarity in selection pressures within step with our dataset.

Heterogeneity within steps of the recombination pathway motivates a more careful investigation of the specific role of genes in the pathway.

Signatures of Selection:

Many gene (~50%) have evidence of negative selection in primates – diagnosed by an excess of non-synonymous polymorphisms in human populations. These results highlight a pattern of conservation among recombination genes.

This approach identifies patterns of selection at the level of the entire gene and positive selection is often thought to target certain domains within proteins. For example, the majority of PRDM9 sequence is conserved and the signature of rapid divergence is constrained to a specific domain. Phylogenetic comparative methods leverage more sequences to allow a more sensitive test for sites of selection.

A sizable fraction of the recombination genes we analyzed (~1/3) showed evidence for positive selection at a subset of sites. These genes are predominantly found in two steps of the pathway:

- (1) genes that form the synaptonemal complex

- (2) the genes that regulate the first steps of the crossover vs. non-crossover decision

PAML has been shown to be susceptible to false positives when assumptions are violated. One potentially pervasive issue are multi-nucleotide mutations, which violate the assumption that the probability of two simultaneous mutations in a single codon is zero.

It is not possible to directly identify MNMs in our dataset, so we choose a highly conservative approach of removing all codons that are inferred to have accumulated multiple mutations on a single branch in the phylogeny. Codons removed using this approach could be MNMs, but they also likely include codons that:

- have accumulated sequential mutations along the long branches in the mammalian phylogeny.
- are neither MNMs or CMDs, due to uncertainty in the inference of ancestral sequences.

Despite the conservative nature of this approach, we still found a signature of positive selection in TEX11 even when all putative CMDs were removed. While this result suggests that MNMs are unlikely to have produced an erroneous signature of selection in TEX11, the conservative nature of the filter makes it difficult to draw conclusions about the nature of the signals of selection in the other recombination genes. It is always to prudent to consider the possibility that relaxed selection has led to elevated rates of evolution.

Observations about specific recombination genes:

The population genetic patterns, paired with knowledge of the molecular function, nominate TEX11 as a very interesting candidate for further investigation: TEX11 exhibits rapid evolution and a robust signature of positive selection.

- TEX11 is the most rapidly evolving recombination gene within primates and across mammals.
- TEX11 exhibits a robust signature of positive selection across mammals.
- 14 residues distributed throughout TEX11 exhibit signatures of positive selection.
- TEX11 is the only gene we surveyed that had more non-synonymous substitutions than non-synonymous polymorphisms.

TEX11 is known to directly interact with of two of the three other genes that evolve most rapidly across the mammalian phylogeny (SHOC1, SYCP2).

Rate correlations among TEX11-SYCP2-SHOC1 are higher than expected from rate correlations among recombination genes – evidence of correlated evolution. This correlation suggests that either:

- (1) all three genes experience concordant selection pressures due to their closely-related functions in the recombination pathway

- (2) rapid evolution of TEX11 is driving compensatory changes in two proteins with which it directly interacts (SYCP2 & SHOC1).

TEX11 is thought to function by binding to the synaptonemal complex (SYCP2) and recruit factors that regulate the first step of the crossover vs. non-crossover decision (SHOC1).

- TEX11 has 3 TRP domains (Guiraldelli *et al.* 2018) and most of the residues with signatures of selection localize to two of the domains – one of which is known to bind to SHOC1.
- "a TRP-like domain, a ubiquitous protein interaction domain that adopts a modular antiparallel array of α-helices"

Caveats:

- (1) genes without signatures of positive selection may contribute to species differences in recombination rate, and genes with evidence of positive selection may not contribute;
- (2) we did not consider all genes in the recombination pathway, nor did we consider the evolution of non-coding sequences

Other Notable Patterns:

IHO1 is also a very interesting gene:

- IHO1 evolves rapidly and has a signature of positive selection.
- IHO1 is a recently discovered gene that is required for DSB formation, it recruits and activated SPO11, a topoisomerase-like gene that generates DSBs.

The genes that are most highly conserved across mammals are exclusively involved in the detection and processing of DSBs. Some of these genes function in DSB detection and repair which may exert non-recombination related selection pressures, however, meiosis-specific genes are among this group.

Comparisons to other observed patterns:

Highlight comparisons to genes specifically mentioned in the introduction:

We do not observe any recombination genes with as extreme a pattern of divergence as PRDM9. However, TEX11 comes close.

- Most of the PRDM9 allele is highly conserved. The zinc-finger domains are highly divergent. 28 of 36 ZF residues differ between human and chimpanzee. 32 sites with evidence of positive selection (dN/dS

406 >> 1). (Thomas *et al.* 2009)

407 MCMDC2 - homolog of MEI-217/MEI-218 - contrasting patterns highlight differences between *Drosophila*
408 and mammals.

Table 1 : List of 32 recombination genes surveyed by step in the recombination pathway. Genes in bold have been associated with inter-individual differences in recombination rate in at least one species of mammals.

Pathway Step	**Genes**
DSB Formation	*HORMAD1, IHO1, MEI4, SPO11,* ***REC114***
DSB Processing	*BRCC3, HORMAD2, MRE11, NBS1, RAD50*
Strand Invasion	*DMC1, MEIOB, MCMDC2, SPATA22, RAD51*
Homologous Pairing	*SYCP1, SYCP2,* ***RAD21L***, ***REC8***, *TEX12*
CO vs. NCO Decision	***MSH4***, ***MSH5***, ***RNF212***, ***RNF212B***, ***TEX11***, *SHOC1*
Resolution	*CNTD1,* ***HEI10***, ***MER3***, *MLH1,* ***MLH3***, *MUS81*

Table 2: Six PAML site models used to measure evolutionary rate and test for positive selection. Models varied in the number of ω classes, the range of ω for each of these classes, and whether a class of sites subject to positive selection was included.

Model	**# Site Classes**	**ω Range**	**Pos. Selection?**
0	1	<1	No
1	2	<1, =1	No
2	3	<1, =1, >1	Yes
7	10	0-1	No
8	11	0-1, >1	Yes
8a	6	0-1, =1	No

414 **Figure 1**: Species tree assumed in analyses of molecular evolution.

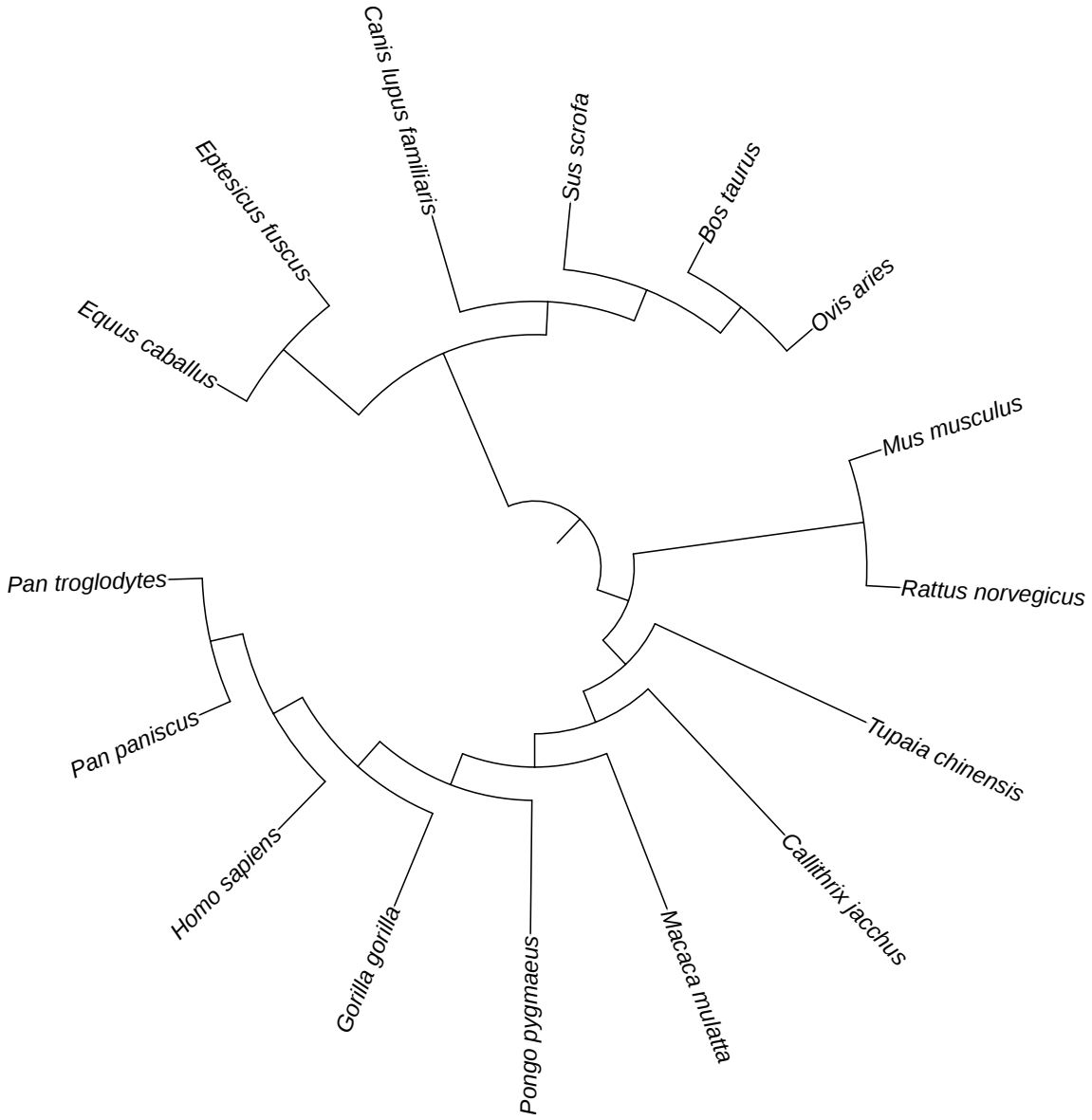

415

Figure 2:Distribution of ω for 32 recombination genes. Bar shows the mean +/- 1 standard deviation. (A) Divergence estimated across the mammalian phylogeny. (B) Pairwise divergence between human and macaque.

(A)

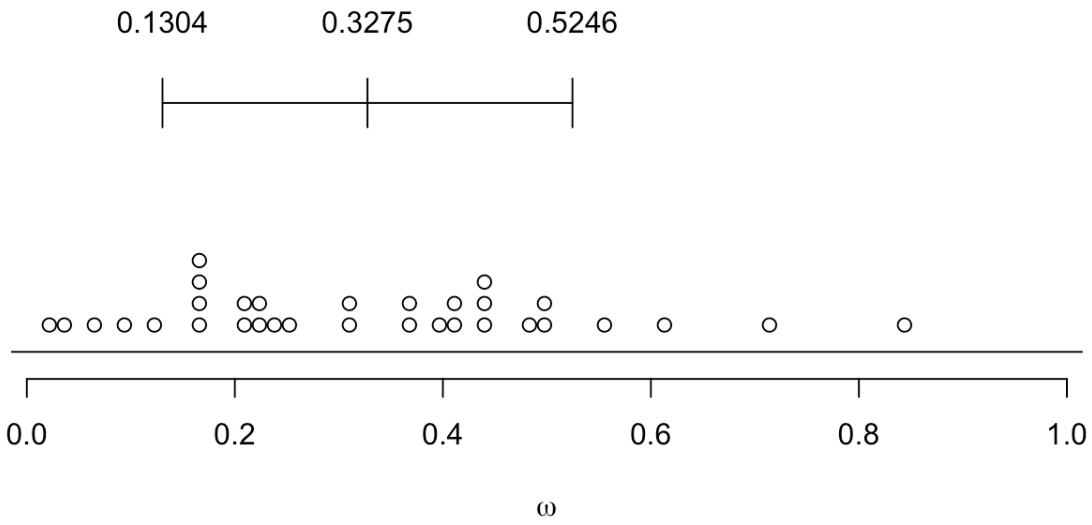

(B)

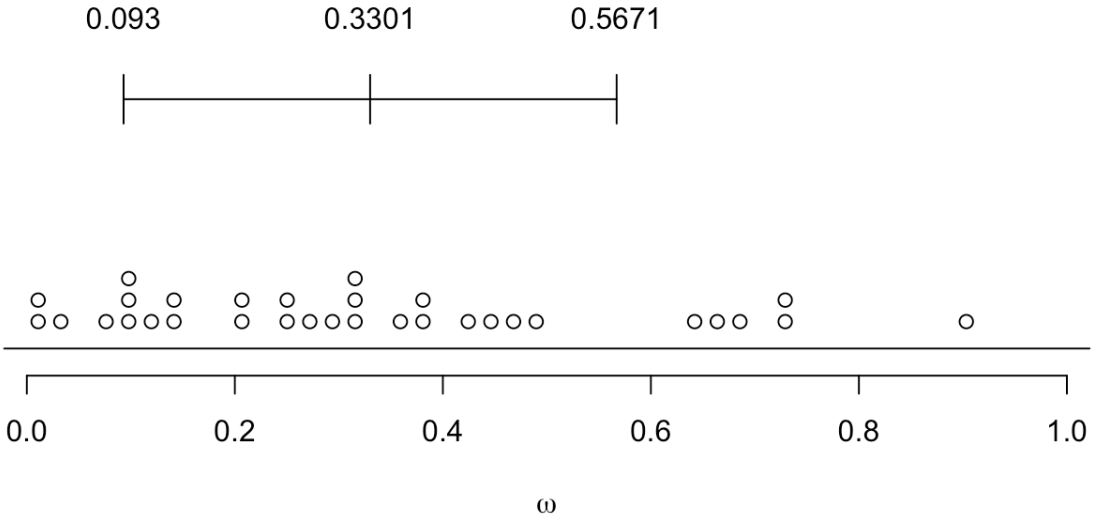

Figure 3: **Pathway Figure Description** The color of each gene represents its evolutionary rate relative to the average rate of evolution of recombination genes ($\omega = 0.3275$): more rapidly evolving genes are depicted in darker shades of red and the more conserved genes are depicted in darker shades of blue. Genes that exhibit a signature of positive selection are in bold.

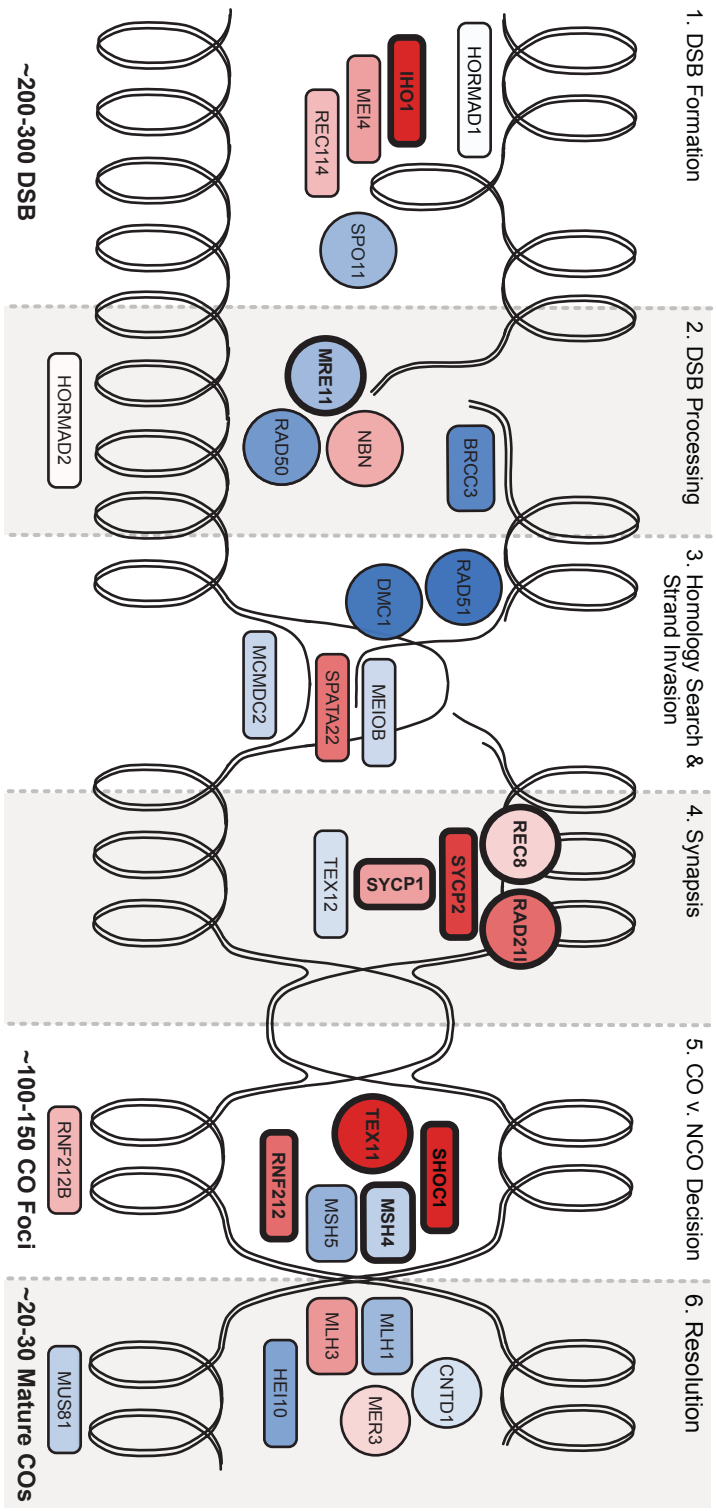
1. DSB Formation
2. DSB Processing
3. Homology Search & Strand Invasion
4. Synapsis
5. CO v. NCO Decision
6. Resolution
HORMAD1
IHO1
MEI4
REC114
SPO11
~200-300 DSB
MRE11
RAD50
NBN
BRCC3
HORMAD2
RAD51
DMC1
MCMDC2
SPATA22
MEIOB
REC8
RAD21L
SYCP2
SYCP1
TEX12
~100-150 CO Foci
TEX11
SHOC1
MSH4
MSH5
RNF212
RNF212B
CNTD1
MER3
MLH1
MLH3
HEI10
~20-30 Mature COs
MUS81

427

Figure 4: Distribution of the mean divergence (ω) between human and macaque of 10,000 random draws from the entire genome. Mean ω among these random draws was observed to be equal to or greater than that observed among recombination genes less than 1% of the time ($p = 0.0075$, 10,000 random draws).

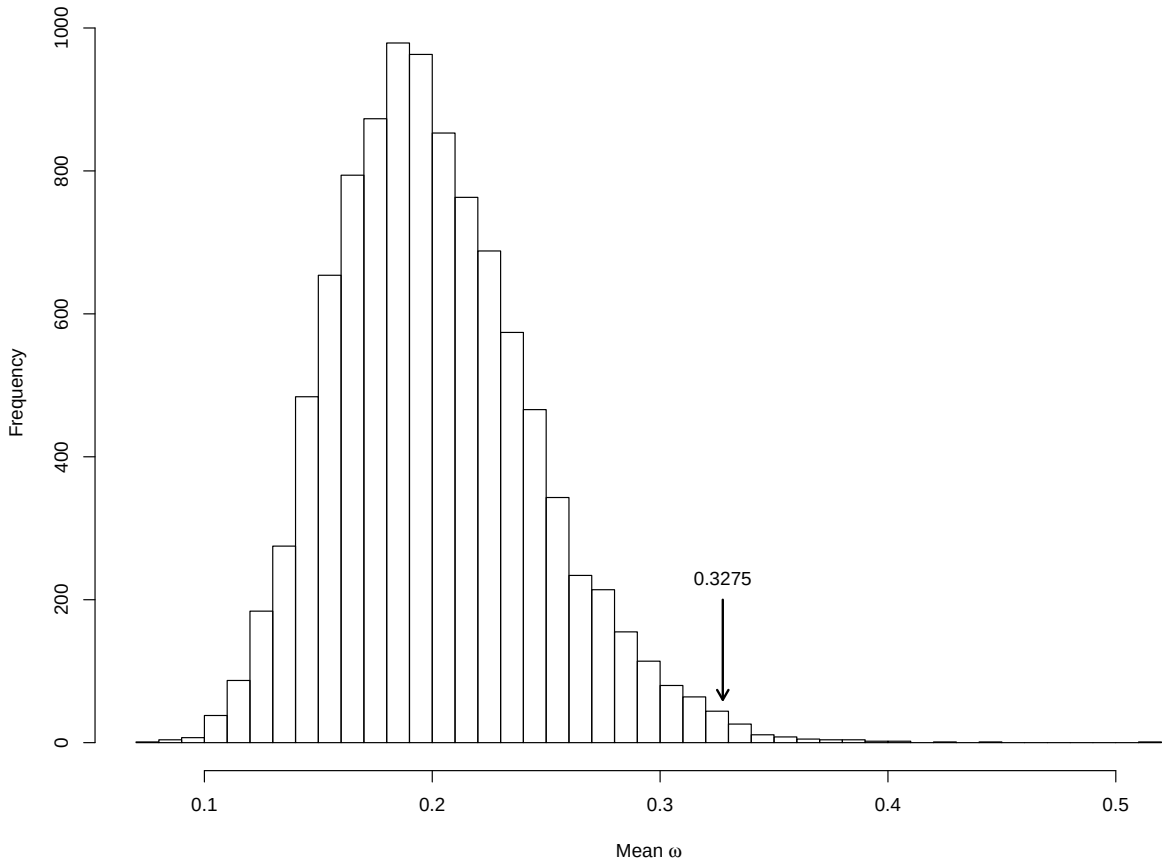

Figure 5: High concordance between there rate of evolution of recombination gene between human and macaques and the rate of evolution among mammals. The linear regression is shown in red and the 1:1 line is shown as a dashed line.

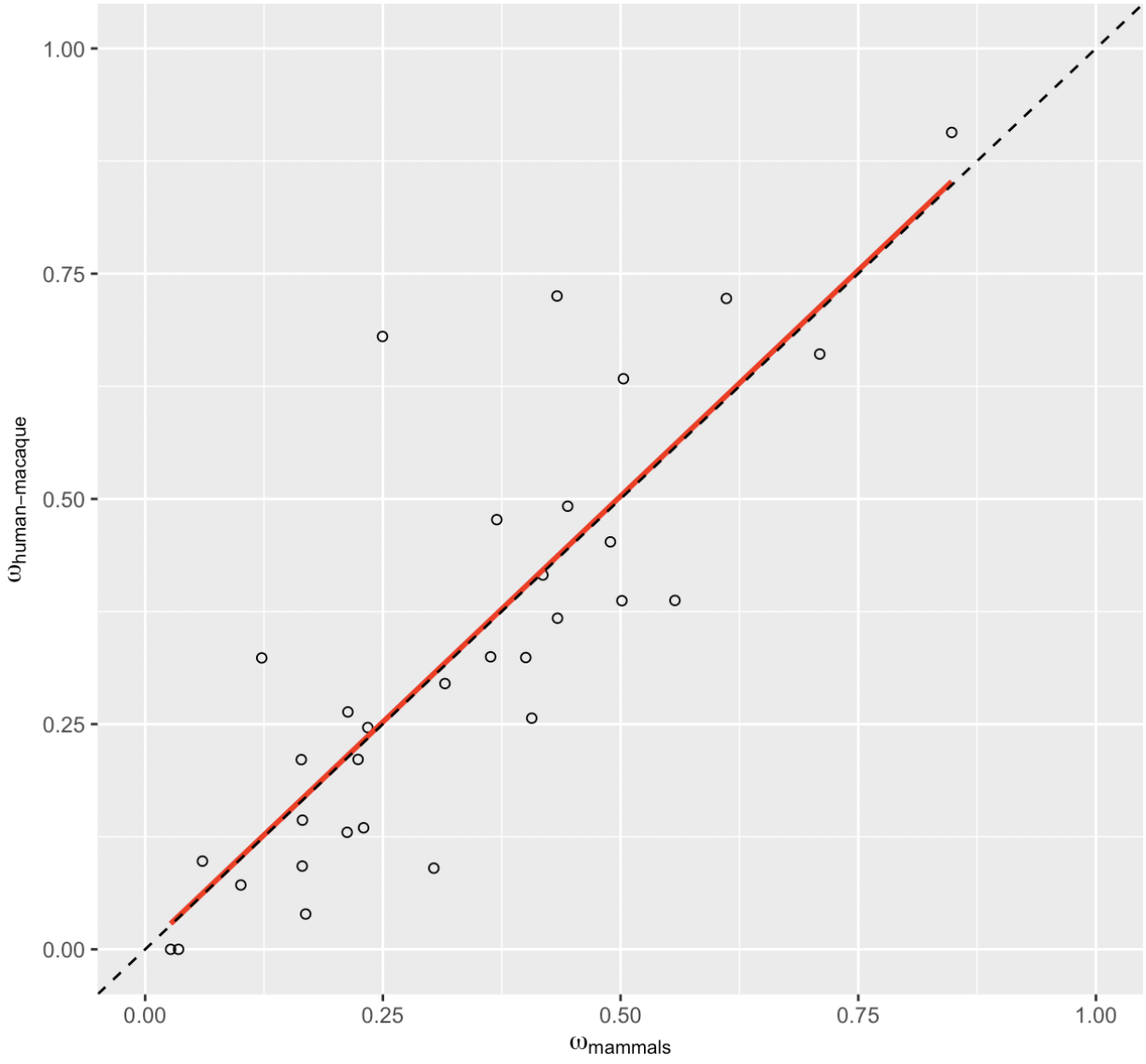

Figure 6: Boxplot of ω by step in recombination pathway.

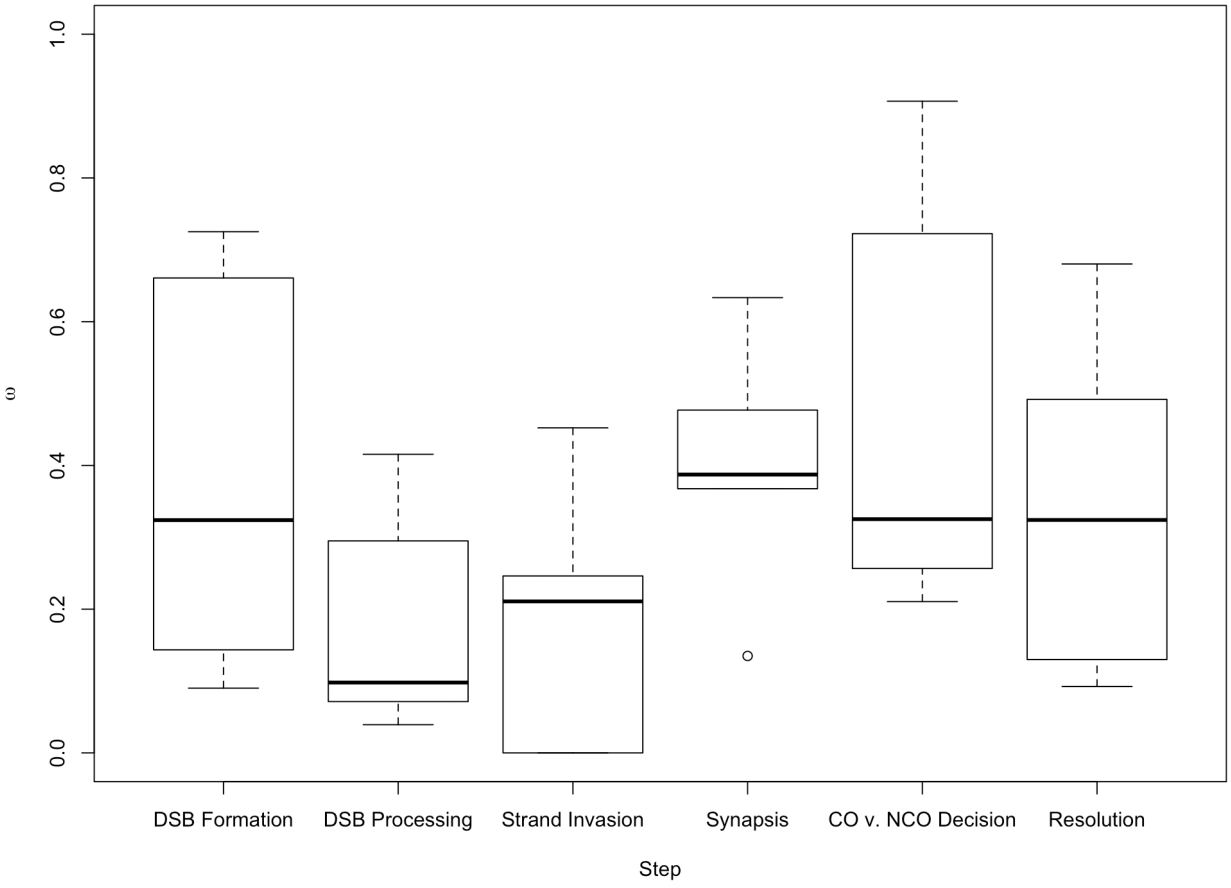

Table 3: PAML analysis of 32 recombination genes in mammals (Yang 2007).

Gene	***bp***	***N***	ω	***M***	***M1-M2***	***p-value***	***M7-M8***	***p-value***	***M8a-M8***	***p-value***	***BEB***
A)											
HORMAD1	1212	16	0.3036	7	0	*1.000*	1.795	*0.4076*	—	—	0
MEI4	1170	16	0.4332	7	0	*1.000*	0.005	*0.9976*	—	—	0
REC114	870	15	0.4003	7	0	*1.000*	5.384	*0.0677*	—	—	0
IHO1	1824	16	0.7095	**8**	13.061	***0.0015***	17.571	***0.0002***	14.527	***0.0001***	**1**
SPO11	1188	15	0.1654	7	0	*1.000*	4.648	*0.0980*	—	—	0
B)											
HORMAD2	981	15	0.3153	7	0	*1.000*	3.650	*0.1612*	—	—	0
MRE11	2136	16	0.1688	**8**	0.363	*0.8342*	11.931	***0.0026***	4.706	***0.0301***	0
NBS1	2289	15	0.4183	**8**	0	*1.000*	12.763	***0.0017***	4.087	***0.0432***	0
RAD50	3936	16	0.1006	7	0	*1.000*	0.301	*0.8605*	—	—-	0
BRCC3	954	15	0.0602	7	0	*1.000*	0.250	*0.8826*	—	—	0
C)											
DMC1	1020	15	0.0351	1	0.488	*0.7835*	5.000	*0.0821*	—	—	**1**
RAD51	1017	16	0.0268	7	0	*1.000*	0	*1.000*	—	—	0
SPATA22	1101	16	0.4893	7	0	*1.000*	0.429	*0.8070*	—	—	0
MEIOB	1425	16	0.2341	7	0	*1.000*	0.665	*0.7172*	—	—	0
MCMDC2	2052	16	0.2239	7	0	*1.000*	0.628	*0.7307*	—	—	0
D)											
REC8	1833	16	0.3698	**8**	0	*1.000*	14.690	***0.0006***	5.927	***0.0149***	0
RAD21L	1686	15	0.503	**8**	12.124	***0.0023***	32.050	***>0.0001***	12.049	***0.0005***	**4**
SYCP1	3015	16	0.4337	**8**	8.711	***0.0128***	26.860	***>0.0001***	9.243	***0.0024***	**3**
SYCP2	4650	16	0.5572	**8**	11.584	***0.0031***	37.200	***>0.0001***	15.838	***0.0001***	0
TEX12	369	14	0.2297	7	0.0565	*0.9721*	1.549	*0.4610*	—	—	0
E)											
TEX11	2844	15	0.8483	**8**	60.872	***>0.0001***	82.665	***>0.0001***	61.141	***>0.0001***	**14**
SHOC1	4644	16	0.6113	**8**	12.447	***0.0020***	30.561	***>0.0001***	15.645	***0.0001***	0
RNF212	948	16	0.5014	**8**	0	*1.000*	16.366	***0.0003***	5.202	***0.0226***	**1**
RNF212B	906	14	0.4066	7	0	*1.000*	0.500	*0.7788*	—	—	0
MSH4	2814	16	0.2132	**8**	16.608	***0.0002***	39.447	***>0.0001***	23.238	***>0.0001***	**6**

Gene	***bp***	***N***	ω	***M***	***M1-M2***	***p-value***	***M7-M8***	***p-value***	***M8a-M8***	***p-value***	***BEB***
MSH5	2565	15	0.1642	7	0	*1.000*	4.214	*0.1216*	—	—	0
F)											
MER3	4458	16	0.3633	8a	0	*1.000*	12.838	***0.0016***	3.109	*0.0779*	0
CNTD1	1026	15	0.2496	7	0	*1.000*	0.936	*0.6263*	—	—	0
HEI10	831	15	0.1226	7	0	*1.000*	0.250	*0.8826*	—	—	0
MLH1	2313	15	0.1652	8a	0	*1.000*	12.221	***0.0022***	0.280	*0.5970*	0
MLH3	4419	16	0.4444	7	0	*1.000*	3.757	*0.1528*	—	—	0
MUS81	1665	16	0.2124	7	0	*1.000*	0.628	*0.7304*	—	—	0

Table 4: PAML - MNM Analysis

Gene	***bp***	***N***	ω	***M***	***M1-M2***	***p-value***	***M7-M8***	***p-value***	***M8a-M8***	***p-value***
IHO1	1824	16	0.6104	7	0	*1.000*	0.258	*0.8789*	—	—
MRE11	2136	16	0.1330	7	0.226	*0.8930*	3.056	*0.2169*	—	—
NBS1	2289	15	0.3413	7	0	*1.000*	1.956	*0.3761*	—	—
REC8	1833	16	0.2905	7	0	*1.000*	5.321	*0.0699*	—	—
RAD21L	1686	15	0.4271	8a	2.329	*0.3121*	9.497	***0.0087***	1.620	*0.2031*
SYCP1	3015	16	0.3731	8a	3.328	*0.1893*	13.440	***0.0012***	2.122	*0.1452*
SYCP2	4650	16	0.4752	7	0	*1.000*	1.758	*0.4151*	—	—
TEX11	2844	15	0.7287	**8**	9.989	***0.0068***	18.776	***0.0001***	10.656	***0.0011***
SHOC1	4644	16	0.5519	8a	0	*1.000*	7.439	***0.0242***	0.292	*0.5887*
RNF212	948	16	0.3685	7	0	*1.000*	0	*1.000*	—	—
MSH4	2814	16	0.1509	7	0	*1.000*	2.079	*0.3536*	—	—

Table 5: Polymorphism & Divergence Data

Gene	ω	***Pn***	***Ps***	***Pn/Ps***	***Dn***	***Ds***	***Dn/Ds***	***MK Test***	***NI***	***DoS***	
A)											
HORMAD1	0.0901	43	10	4.3	5	12	0.4167	***0.0002***	10.32	-0.5172	Neg.
MEI4	0.7252	9	2	4.5	24	9	2.6667	*0.7013*	1.6875	-0.0909	—
REC114	0.3239	49	21	2.3333	11	14	0.7857	***0.02949***	2.9700	-0.2600	Neg.
IHO1	0.6608	72	28	2.5714	36	19	1.8947	*0.4658*	1.3571	-0.0645	—
SPO11	0.1434	62	28	2.2143	11	22	0.5000	***0.0008***	4.4286	-0.3556	Neg.
B)											
HORMAD2	0.295	50	16	3.125	7	9	0.7778	***0.0177***	4.0179	-0.3201	Neg.
MRE11	0.0392	139	48	2.8958	5	35	0.1429	***>0.0001***	20.2708	-0.6183	Neg.
NBS1	0.4155	119	58	2.0517	34	25	1.3600	*0.2086*	1.5086	-0.0960	—
RAD50	0.0714	168	55	3.0517	8	43	0.1860	***>0.0001***	16.4182	-0.5965	Neg.
BRCC3	0.0979	7	12	0.5833	2	6	0.3333	*0.6758*	1.7500	-0.1184	—
C)											
DMC1	0.000	43	25	1.72	0	11	0.0000	***<0.0001***	—	-0.6324	Neg.
RAD51	0.000	27	29	0.9310	0	13	0.0000	***0.0010***	—	-0.4821	Neg.
SPATA22	0.4523	67	26	2.5769	21	10	2.1000	*0.6535*	1.2271	-0.0430	—
MEIOB	0.2462	45	17	2.6471	20	22	0.9091	***0.0094***	2.9118	-0.2496	Neg.
MCMDC2	0.2108	90	24	3.7500	16	26	0.6154	***<0.0001***	6.0938	-0.4085	Neg.
D)											
REC8	0.477	90	45	2.000	38	31	1.2258	*0.1264*	1.6316	-0.1159	—
RAD21L	0.6334	21	6	3.500	27	13	2.0769	*0.4176*	1.6852	-0.1028	—
SYCP1	0.3676	122	60	2.033	33	37	1.2222	*0.1204*	1.6636	-0.1203	—
SYCP2	0.3676	246	87	2.8276	74	53	1.3962	***0.0015***	2.0252	-0.1561	Neg.
TEX12	0.1349	15	9	1.6667	2	4	0.5000	*0.3598*	3.3333	-0.2917	—
E)											
TEX11	0.9068	78	45	1.7333	55	25	2.200	*0.4541*	0.7879	0.05335	—
SHOC1	0.7225	227	72	3.1528	85	37	2.2973	*0.2199*	1.3724	-0.0625	—
RNF212	0.387	—	—	—	17	18	0.9444	—	—	—	—
RNF212B	0.2566	9	3	3.000	8	12	0.6667	*0.0759*	4.5000	-0.3500	—
MSH4	0.2635	149	50	2.9800	24	29	0.8276	***<0.0001***	3.6008	-0.2959	Neg.

Gene	ω	***Pn***	***Ps***	***Pn/Ps***	***Dn***	***Ds***	***Dn/Ds***	***MK Test***	***NI***	***DoS***	
MSH5	0.2106	129	64	2.0156	19	33	0.5758	***0.0001***	3.5008	-0.3030	Neg.
F)											
MER3	0.3247	236	92	2.5652	54	44	1.2273	***0.0029***	2.0902	-0.1685	Neg.
CNTD1	0.6803	56	29	1.9310	13	8	1.6250	*0.8001*	1.1883	-0.0398	—
HEI10	0.3235	50	21	2.3810	4	5	0.8000	*0.1417*	2.9762	-0.2598	—
MLH1	0.0924	161	48	3.3542	9	29	0.3103	***>0.0001***	10.8079	-0.5335	Neg.
MLH3	0.4919	252	90	2.8	77	57	1.3509	***0.0009***	2.0727	-0.1622	Neg.
MUS81	0.1299	129	49	2.6327	17	40	0.4250	***>0.0001***	6.1945	-0.4265	Neg.

Acknowledgements

We thank Nathan Clark for assistance with evolutionary covariation rate analyses. A.L.D. was supported by NHGRI Training Grant to the Genomic Sciences Training Program 5T32HG002760. B.A.P. was supported by NIH grant NIH grant R01 GM120051.

References

Abascal F., R. Zardoya, and M. J. Telford, 2010 TranslatorX: Multiple alignment of nucleotide sequences guided by amino acid translations. Nucleic acids research 38: W7–W13.

Baker S. M., A. W. Plug, T. A. Prolla, C. E. Bronner, and A. C. Harris *et al.*, 1996 Involvement of mouse mlh1 in dna mismatch repair and meiotic crossing over. Nature genetics 13: 336.

Balcova M., B. Faltusova, V. Gergelits, T. Bhattacharyya, and O. Mihola *et al.*, 2016 Hybrid sterility locus on chromosome x controls meiotic recombination rate in mouse. PLoS genetics 12: e1005906.

Barbosa-Morais N. L., M. Irimia, Q. Pan, H. Y. Xiong, and S. Gueroussov *et al.*, 2012 The evolutionary landscape of alternative splicing in vertebrate species. Science 338: 1587–1593.

Barrett T., S. E. Wilhite, P. Ledoux, C. Evangelista, and I. F. Kim *et al.*, 2012 NCBI geo: Archive for functional genomics data sets—update. Nucleic acids research 41: D991–D995.

Baudat F., K. Manova, J. P. Yuen, M. Jasin, and S. Keeney, 2000 Chromosome synapsis defects and sexually dimorphic meiotic progression in mice lacking spo11. Molecular cell 6: 989–998.

Baudat F., and B. de Massy, 2007 Regulating double-stranded dna break repair towards crossover or non-crossover during mammalian meiosis. Chromosome research 15: 565–577.

Begun D. J., and C. F. Aquadro, 1992 Levels of naturally occurring dna polymorphism correlate with recombination rates in d. Melanogaster. Nature 356: 519.

Bergerat A., B. de Massy, D. Gadelle, P.-C. Varoutas, and A. Nicolas *et al.*, 1997 An atypical topoisomerase ii from archaea with implications for meiotic recombination. Nature 386: 414.

Besenbacher S., P. Sulem, A. Helgason, H. Helgason, and H. Kristjansson *et al.*, 2016 Multi-nucleotide de novo mutations in humans. PLoS genetics 12: e1006315.

Bisig C. G., M. F. Guiraldelli, A. Kouznetsova, H. Scherthan, and C. Höög *et al.*, 2012 Synaptonemal complex components persist at centromeres and are required for homologous centromere pairing in mouse

spermatocytes. PLoS genetics 8: e1002701.

Bolcun-Filas E., and J. C. Schimenti, 2012 Genetics of meiosis and recombination in mice. International review of cell and molecular biology 298: 179–227.

Brand C. L., M. V. Cattani, S. B. Kingan, E. L. Landeen, and D. C. Presgraves, 2018 Molecular evolution at a meiosis gene mediates species differences in the rate and patterning of recombination. Current Biology 28: 1289–1295.

Broman K. W., J. C. Murray, V. C. Sheffield, R. L. White, and J. L. Weber, 1998 Comprehensive human genetic maps: Individual and sex-specific variation in recombination. The American Journal of Human Genetics 63: 861–869.

Brown M. S., and D. K. Bishop, 2014 DNA strand exchange and reca homologs in meiosis. Cold Spring Harbor perspectives in biology a016659.

Burt A., and G. Bell, 1987 Red queen versus tangled bank models. Nature 330: 118.

Charlesworth B., M. Morgan, and D. Charlesworth, 1993 The effect of deleterious mutations on neutral molecular variation. Genetics 134: 1289–1303.

Charlesworth B., 1994 The effect of background selection against deleterious mutations on weakly selected, linked variants. Genetics Research 63: 213–227.

Charlesworth B., P. Jarne, and S. Assimacopoulos, 1994 The distribution of transposable elements within and between chromosomes in a population of drosophila melanogaster. III. Element abundances in heterochromatin. Genetics Research 64: 183–197.

Chen M.-Y., D. Liang, and P. Zhang, 2017 Phylogenomic resolution of the phylogeny of laurasiatherian mammals: Exploring phylogenetic signals within coding and noncoding sequences. Genome biology and evolution 9: 1998–2012.

Chowdhury R., P. R. Bois, E. Feingold, S. L. Sherman, and V. G. Cheung, 2009 Genetic analysis of variation in human meiotic recombination. PLoS genetics 5: e1000648.

Clark N. L., J. Gasper, M. Sekino, S. A. Springer, and C. F. Aquadro *et al.*, 2009 Coevolution of interacting fertilization proteins. PLoS genetics 5: e1000570.

Clark N. L., E. Alani, and C. F. Aquadro, 2012 Evolutionary rate covariation reveals shared functionality and coexpression of genes. Genome research.

Clark N. L., E. Alani, and C. F. Aquadro, 2013 Evolutionary rate covariation in meiotic proteins results from fluctuating evolutionary pressure in yeasts and mammals. Genetics 193: 529–538.

Cloud V., Y.-L. Chan, J. Grubb, B. Budke, and D. K. Bishop, 2012 Rad51 is an accessory factor for dmc1-mediated joint molecule formation during meiosis. Science 337: 1222–1225.

Comeron J. M., M. Kreitman, and M. Aguadé, 1999 Natural selection on synonymous sites is correlated with gene length and recombination in drosophila. Genetics 151: 239–249.

Comeron J. M., R. Ratnappan, and S. Bailin, 2012 The many landscapes of recombination in drosophila melanogaster. PLoS genetics 8: e1002905.

Coop G., and M. Przeworski, 2007 An evolutionary view of human recombination. Nature Reviews Genetics 8: 23.

Costa Y., R. Speed, R. Öllinger, M. Alsheimer, and C. A. Semple *et al.*, 2005 Two novel proteins recruited by synaptonemal complex protein 1 (sycp1) are at the centre of meiosis. Journal of cell science 118: 2755–2762.

Dapper A. L., and B. A. Payseur, 2017 Connecting theory and data to understand recombination rate evolution. Phil. Trans. R. Soc. B 372: 20160469.

Dumont B. L., and B. A. Payseur, 2010 Evolution of the genomic recombination rate in murid rodents. Genetics.

Dumont B. L., M. A. White, B. Steffy, T. Wiltshire, and B. A. Payseur, 2011 Extensive recombination rate variation in the house mouse species complex inferred from genetic linkage maps. Genome research 21: 114–125.

Duret L., and P. F. Arndt, 2008 The impact of recombination on nucleotide substitutions in the human genome. PLoS genetics 4: e1000071.

Edelmann W., P. E. Cohen, M. Kane, K. Lau, and B. Morrow *et al.*, 1996 Meiotic pachytene arrest in mlh1-deficient mice. Cell 85: 1125–1134.

Edgar R. C., 2004 MUSCLE: Multiple sequence alignment with high accuracy and high throughput. Nucleic acids research 32: 1792–1797.

Fan Y., Z.-Y. Huang, C.-C. Cao, C.-S. Chen, and Y.-X. Chen *et al.*, 2013 Genome of the chinese tree shrew. Nature communications 4: 1426.

Fay J. C., G. J. Wyckoff, and C.-I. Wu, 2001 Positive and negative selection on the human genome. Genetics 158: 1227–1234.

Felsenstein J., 1974 The evolutionary advantage of recombination. Genetics 78: 737–756.

Finsterbusch F., R. Ravindranathan, I. Dereli, M. Stanzione, and D. Tränkner *et al.*, 2016 Alignment of homologous chromosomes and effective repair of programmed dna double-strand breaks during mouse meiosis require the minichromosome maintenance domain containing 2 (mcmdc2) protein. PLoS genetics 12: e1006393.

Fledel-Alon A., E. M. Leffler, Y. Guan, M. Stephens, and G. Coop *et al.*, 2011 Variation in human recombination rates and its genetic determinants. PloS one 6: e20321.

Fraune J., M. Alsheimer, J. Redolfi, C. Brochier-Armanet, and R. Benavente, 2014 Protein sycp2 is an ancient component of the metazoan synaptonemal complex. Cytogenetic and genome research 144: 299–305.

Gonen S., M. Battagin, S. E. Johnston, G. Gorjanc, and J. M. Hickey, 2017 The potential of shifting recombination hotspots to increase genetic gain in livestock breeding. Genetics Selection Evolution 49: 55.

Grey C., P. Barthès, Chauveau-Le FriecG., F. Langa, and F. Baudat *et al.*, 2011 Mouse prdm9 dna-binding specificity determines sites of histone h3 lysine 4 trimethylation for initiation of meiotic recombination. PLoS biology 9: e1001176.

Grey C., F. Baudat, and B. de Massy, 2018 PRDM9, a driver of the genetic map. PLoS genetics 14: e1007479.

Guiraldelli M. F., A. Felberg, L. P. Almeida, A. Parikh, and R. O. de Castro *et al.*, 2018 SHOC1 is a ercc4-(hhh) 2-like protein, integral to the formation of crossover recombination intermediates during mammalian meiosis. PLoS genetics 14: e1007381.

Hakes L., S. C. Lovell, S. G. Oliver, and D. L. Robertson, 2007 Specificity in protein interactions and its relationship with sequence diversity and coevolution. Proceedings of the National Academy of Sciences 104: 7999–8004.

Hamer G., K. Gell, A. Kouznetsova, I. Novak, and R. Benavente *et al.*, 2006 Characterization of a novel meiosis-specific protein within the central element of the synaptonemal complex. Journal of cell science 119: 4025–4032.

Hassold T., and P. Hunt, 2001 To err (meiotically) is human: The genesis of human aneuploidy. Nature Reviews Genetics 2: 280.

Hernández-Hernández A., S. Masich, T. Fukuda, A. Kouznetsova, and S. Sandin *et al.*, 2016 The central element of the synaptonemal complex in mice is organized as a bilayered junction structure. J Cell Sci 129: 2239–2249.

Hill W. G., and A. Robertson, 1966 The effect of linkage on limits to artificial selection. Genetics Research 8: 269–294.

Hunter C. M., W. Huang, T. F. Mackay, and N. D. Singh, 2016 The genetic architecture of natural variation in recombination rate in drosophila melanogaster. PLoS genetics 12: e1005951.

Jeffreys A. J., R. Neumann, M. Panayi, S. Myers, and P. Donnelly, 2005 Human recombination hot spots hidden in regions of strong marker association. Nature genetics 37: 601.

Johnston S. E., C. Bérénos, J. Slate, and J. M. Pemberton, 2016 Conserved genetic architecture underlying individual recombination rate variation in a wild population of soay sheep (ovis aries). Genetics genetics–115.

Johnston S. E., J. Huisman, and J. M. Pemberton, 2018 A genomic region containing rec8 and rnf212b is associated with individual recombination rate variation in a wild population of red deer (cervus elaphus). G3: Genes, Genomes, Genetics g3–200063.

Kadri N. K., C. Harland, P. Faux, N. Cambisano, and L. Karim *et al.*, 2016 Coding and noncoding variants in hfm1, mlh3, msh4, msh5, rnf212, and rnf212b affect recombination rate in cattle. Genome research.

Keeney S., C. N. Giroux, and N. Kleckner, 1997 Meiosis-specific dna double-strand breaks are catalyzed by spo11, a member of a widely conserved protein family. Cell 88: 375–384.

Keeney S., 2007 Spo11 and the formation of dna double-strand breaks in meiosis, pp. 81–123 in *Recombination and meiosis*, Springer.

Kobayashi W., M. Takaku, S. Machida, H. Tachiwana, and K. Maehara *et al.*, 2016 Chromatin architecture may dictate the target site for dmc1, but not for rad51, during homologous pairing. Scientific reports 6: 24228.

Kong A., G. Thorleifsson, H. Stefansson, G. Masson, and A. Helgason *et al.*, 2008 Sequence variants in the rnf212 gene associate with genome-wide recombination rate. Science 319: 1398–1401.

Kong A., G. Thorleifsson, D. F. Gudbjartsson, G. Masson, and A. Sigurdsson *et al.*, 2010 Fine-scale recombination rate differences between sexes, populations and individuals. Nature 467: 1099.

Kong A., G. Thorleifsson, M. L. Frigge, G. Masson, and D. F. Gudbjartsson *et al.*, 2014 Common and low-frequency variants associated with genome-wide recombination rate. Nature genetics 46: 11.

Kumar R., N. Ghyselinck, K.-i. Ishiguro, Y. Watanabe, and A. Kouznetsova *et al.*, 2015 MEI4: A central player in the regulation of meiotic dna double strand break formation in the mouse. J Cell Sci jcs–165464.

Lange J., S. Yamada, S. E. Tischfield, J. Pan, and S. Kim *et al.*, 2016 The landscape of mouse meiotic double-strand break formation, processing, and repair. Cell 167: 695–708.

Langmead B., and S. L. Salzberg, 2012 Fast gapped-read alignment with bowtie 2. Nature methods 9: 357.

La Salle S., K. Palmer, O'BrienM., J. C. Schimenti, and J. Eppig *et al.*, 2012 Spata22, a novel vertebrate-specific gene, is required for meiotic progress in mouse germ cells. Biology of reproduction 86: 45–1.

Latrille T., L. Duret, and N. Lartillot, 2017 The red queen model of recombination hot-spot evolution: A theoretical investigation. Phil. Trans. R. Soc. B 372: 20160463.

Leinonen R., H. Sugawara, M. Shumway, and I. N. S. D. Collaboration, 2010 The sequence read archive. Nucleic acids research 39: D19–D21.

Lek M., K. J. Karczewski, E. V. Minikel, K. E. Samocha, and E. Banks *et al.*, 2016 Analysis of protein-coding genetic variation in 60,706 humans. Nature 536: 285.

Lesecque Y., S. Glémin, N. Lartillot, D. Mouchiroud, and L. Duret, 2014 The red queen model of recombination hotspots evolution in the light of archaic and modern human genomes. PLoS genetics 10: e1004790.

Li H., B. Handsaker, A. Wysoker, T. Fennell, and J. Ruan *et al.*, 2009 The sequence alignment/map format and samtools. Bioinformatics 25: 2078–2079.

Lipkin S. M., P. B. Moens, V. Wang, M. Lenzi, and D. Shanmugarajah *et al.*, 2002 Meiotic arrest and aneuploidy in mlh3-deficient mice. Nature genetics 31: 385.

Ma L., O'ConnellJ. R., P. M. VanRaden, B. Shen, and A. Padhi *et al.*, 2015 Cattle sex-specific recombination and genetic control from a large pedigree analysis. PLoS genetics 11: e1005387.

McDonald J. H., and M. Kreitman, 1991 Adaptive protein evolution at the adh locus in drosophila. Nature 351: 652.

Meuwissen R., H. H. Offenberg, A. Dietrich, A. Riesewijk, and M. van Iersel *et al.*, 1992 A coiled-coil related protein specific for synapsed regions of meiotic prophase chromosomes. The EMBO Journal 11: 5091.

Murdoch B., N. Owen, S. Shirley, S. Crumb, and K. W. Broman *et al.*, 2010 Multiple loci contribute to genome-wide recombination levels in male mice. Mammalian genome 21: 550–555.

Myers S., R. Bowden, A. Tumian, R. E. Bontrop, and C. Freeman *et al.*, 2010 Drive against hotspot motifs in primates implicates the prdm9 gene in meiotic recombination. Science 327: 876–879.

Oh J., A. Al-Zain, E. Cannavo, P. Cejka, and L. S. Symington, 2016 Xrs2 dependent and independent

functions of the mre11-rad50 complex. Molecular cell 64: 405–415.

Oliver P. L., L. Goodstadt, J. J. Bayes, Z. Birtle, and K. C. Roach *et al.*, 2009 Accelerated evolution of the prdm9 speciation gene across diverse metazoan taxa. PLoS genetics 5: e1000753.

Pamilo P., and M. Nei, 1988 Relationships between gene trees and species trees. Molecular biology and evolution 5: 568–583.

Pan Q., O. Shai, L. J. Lee, B. J. Frey, and B. J. Blencowe, 2008 Deep surveying of alternative splicing complexity in the human transcriptome by high-throughput sequencing. Nature genetics 40: 1413.

Parvanov E. D., P. M. Petkov, and K. Paigen, 2010 Prdm9 controls activation of mammalian recombination hotspots. Science 327: 835–835.

Pazos F., and A. Valencia, 2001 Similarity of phylogenetic trees as indicator of protein–protein interaction. Protein engineering 14: 609–614.

Perelman P., W. E. Johnson, C. Roos, H. N. Seuánez, and J. E. Horvath *et al.*, 2011 A molecular phylogeny of living primates. PLoS genetics 7: e1001342.

Petit M., J.-M. Astruc, J. Sarry, L. Drouilhet, and S. Fabre *et al.*, 2017 Variation in recombination rate and its genetic determinism in sheep populations. Genetics genetics–300123.

Prasad A. B., M. W. Allard, N. C. S. Program, and E. D. Green, 2008 Confirming the phylogeny of mammals by use of large comparative sequence data sets. Molecular Biology and Evolution 25: 1795–1808.

Priedigkeit N., N. Wolfe, and N. L. Clark, 2015 Evolutionary signatures amongst disease genes permit novel methods for gene prioritization and construction of informative gene-based networks. PLoS genetics 11: e1004967.

Rao H. P., H. Qiao, S. K. Bhatt, L. R. Bailey, and H. D. Tran *et al.*, 2017 A sumo-ubiquitin relay recruits proteasomes to chromosome axes to regulate meiotic recombination. Science 355: 403–407.

Reynolds A., H. Qiao, Y. Yang, J. K. Chen, and N. Jackson *et al.*, 2013 RNF212 is a dosage-sensitive regulator of crossing-over during mammalian meiosis. Nature genetics 45: 269.

Rogacheva M. V., C. M. Manhart, C. Chen, A. Guarne, and J. Surtees *et al.*, 2014 Mlh1-mlh3, a meiotic crossover and dna mismatch repair factor, is a msh2-msh3-stimulated endonuclease. Journal of Biological Chemistry jbc–M113.

Romanienko P. J., and R. D. Camerini-Otero, 2000 The mouse spo11 gene is required for meiotic chromosome synapsis. Molecular cell 6: 975–987.

Ronquist F., M. Teslenko, Van Der MarkP., D. L. Ayres, and A. Darling *et al.*, 2012 MrBayes 3.2: Efficient bayesian phylogenetic inference and model choice across a large model space. Systematic biology 61: 539–542.

Rosenberg N. A., 2002 The probability of topological concordance of gene trees and species trees. Theoretical population biology 61: 225–247.

Sandor C., W. Li, W. Coppieters, T. Druet, and C. Charlier *et al.*, 2012 Genetic variants in rec8, rnf212, and prdm9 influence male recombination in cattle. PLoS genetics 8: e1002854.

Schmekel K., and B. Daneholt, 1995 The central region of the synaptonemal complex revealed in three dimensions. Trends in cell biology 5: 239–242.

Schramm S., J. Fraune, R. Naumann, A. Hernandez-Hernandez, and C. Höög *et al.*, 2011 A novel mouse synaptonemal complex protein is essential for loading of central element proteins, recombination, and fertility. PLoS genetics 7: e1002088.

Schrider D. R., J. N. Hourmozdi, and M. W. Hahn, 2011 Pervasive multinucleotide mutational events in eukaryotes. Current Biology 21: 1051–1054.

Scornavacca C., and N. Galtier, 2017 Incomplete lineage sorting in mammalian phylogenomics. Systematic biology 66: 112–120.

Segura J., L. Ferretti, S. Ramos-Onsins, L. Capilla, and M. Farré *et al.*, 2013 Evolution of recombination in eutherian mammals: Insights into mechanisms that affect recombination rates and crossover interference. Proceedings of the Royal Society of London B: Biological Sciences 280: 20131945.

Shen B., J. Jiang, E. Seroussi, G. E. Liu, and L. Ma, 2018 Characterization of recombination features and the genetic basis in multiple cattle breeds. BMC genomics 19: 304.

Smith N. G., and A. Eyre-Walker, 2002 Adaptive protein evolution in drosophila. Nature 415: 1022.

Smukowski C., and M. Noor, 2011 Recombination rate variation in closely related species. Heredity 107: 496.

Snowden T., S. Acharya, C. Butz, M. Berardini, and R. Fishel, 2004 HMSH4-hMSH5 recognizes holliday junctions and forms a meiosis-specific sliding clamp that embraces homologous chromosomes. Molecular cell 15: 437–451.

Stanzione M., M. Baumann, F. Papanikos, I. Dereli, and J. Lange *et al.*, 2016 Meiotic dna break formation requires the unsynapsed chromosome axis-binding protein iho1 (ccdc36) in mice. Nature cell biology 18: 1208.

Stapley J., P. G. Feulner, S. E. Johnston, A. W. Santure, and C. M. Smadja, 2017 Variation in recombination frequency and distribution across eukaryotes: Patterns and processes. Phil. Trans. R. Soc. B 372: 20160455.

668 Stoletzki N., and A. Eyre-Walker, 2010 Estimation of the neutrality index. Molecular biology and evolution
669 28: 63–70.

670 Thomas J. H., R. O. Emerson, and J. Shendure, 2009 Extraordinary molecular evolution in the prdm9 fertility
671 gene. PloS one 4: e8505.

672 Thorvaldsdóttir H., J. T. Robinson, and J. P. Mesirov, 2013 Integrative genomics viewer (igv): High-
673 performance genomics data visualization and exploration. Briefings in bioinformatics 14: 178–192.

674 Trapnell C., L. Pachter, and S. L. Salzberg, 2009 TopHat: Discovering splice junctions with rna-seq.
675 Bioinformatics 25: 1105–1111.

676 Ubeda F., and J. Wilkins, 2011 The red queen theory of recombination hotspots. Journal of evolutionary
677 biology 24: 541–553.

678 Venkat A., M. W. Hahn, and J. W. Thornton, 2018 Multinucleotide mutations cause false inferences of
679 lineage-specific positive selection. Nature ecology & evolution 2: 1280.

680 Vries S. S. de, E. B. Baart, M. Dekker, A. Siezen, and D. G. de Rooij *et al.*, 1999 Mouse muts-like protein
681 msh5 is required for proper chromosome synapsis in male and female meiosis. Genes & Development 13:
682 523–531.

683 Vries F. A. de, E. de Boer, M. van den Bosch, W. M. Baarends, and M. Ooms *et al.*, 2005 Mouse sycp1
684 functions in synaptonemal complex assembly, meiotic recombination, and xy body formation. Genes &
685 development 19: 1376–1389.

686 Ward J. O., L. G. Reinholdt, W. W. Motley, L. M. Niswander, and D. C. Deacon *et al.*, 2007 Mutation in
687 mouse hei10, an e3 ubiquitin ligase, disrupts meiotic crossing over. PLoS genetics 3: e139.

688 Wheeler D. L., T. Barrett, D. A. Benson, S. H. Bryant, and K. Canese *et al.*, 2006 Database resources of the
689 national center for biotechnology information. Nucleic acids research 35: D5–D12.

690 Xu Y., R. A. Greenberg, E. Schonbrunn, and P. J. Wang, 2017 Meiosis-specific proteins meiob and spata22
691 cooperatively associate with the single-stranded dna-binding replication protein a complex and dna double-
692 strand breaks. Biology of reproduction 96: 1096–1104.

693 Yang Z., 1997 PAML: A program package for phylogenetic analysis by maximum likelihood. Bioinformatics
694 13: 555–556.

695 Yang F., De La FuenteR., N. A. Leu, C. Baumann, and K. J. McLaughlin *et al.*, 2006 Mouse sycp2 is required
696 for synaptonemal complex assembly and chromosomal synapsis during male meiosis. The Journal of Cell

Biology 173: 497–507.

Yang Z., 2007 PAML 4: Phylogenetic analysis by maximum likelihood. Molecular Biology and Evolution 24: 1586–1591. https://doi.org/10.1093/molbev/msm088

Yang F., K. Gell, Van Der HeijdenG. W., S. Eckardt, and N. A. Leu *et al.*, 2008 Meiotic failure in male mice lacking an x-linked factor. Genes & development 22: 682–691.

Zerbino D. R., P. Achuthan, W. Akanni, M. R. Amode, and D. Barrell *et al.*, 2017 Ensembl 2018. Nucleic acids research 46: D754–D761.